



Technological University Dublin  
ARROW@TU Dublin

---

Conference papers

Communications Network Research Institute

---

2021

## A Linear Predictive Coding Filtering Method for Time-resolved Morphology of EEG Activity

Jin Xu

Mark Davis

Ruairí de Fréin

Follow this and additional works at: <https://arrow.tudublin.ie/commcon>

 Part of the [Biomedical Engineering and Bioengineering Commons](#)

---

This Conference Paper is brought to you for free and open access by the Communications Network Research Institute at ARROW@TU Dublin. It has been accepted for inclusion in Conference papers by an authorized administrator of ARROW@TU Dublin. For more information, please contact [arrow.admin@tudublin.ie](mailto:arrow.admin@tudublin.ie), [aisling.coyne@tudublin.ie](mailto:aisling.coyne@tudublin.ie).



This work is licensed under a [Creative Commons Attribution-NonCommercial-Share Alike 3.0 License](#)



---

Articles

---

2021

## A Linear Predictive Coding Filtering Method for Time-resolved Morphology of EEG Activity

Jin Xu

Mark Davis

Ruairí de Fréin

Follow this and additional works at: <https://arrow.tudublin.ie/creaart>



Part of the [Biomedical Engineering and Bioengineering Commons](#), and the [Signal Processing Commons](#)

---

This Conference Paper is brought to you for free and open access by ARROW@TU Dublin. It has been accepted for inclusion in Articles by an authorized administrator of ARROW@TU Dublin. For more information, please contact [arrow.admin@tudublin.ie](mailto:arrow.admin@tudublin.ie), [aisling.coyne@tudublin.ie](mailto:aisling.coyne@tudublin.ie).



This work is licensed under a [Creative Commons Attribution-NonCommercial-Share Alike 3.0 License](#)

# A Linear Predictive Coding Filtering Method for the Time-resolved Morphology of EEG Activity

Jin Xu\*, Mark Davis<sup>†</sup>, and Ruairí de Fréin<sup>‡</sup>

School of Electrical and Electronic Engineering, Technological University Dublin, Ireland

Email: \*D17128410@mytudublin.ie, <sup>†</sup>mark.davis@tudublin.ie, <sup>‡</sup>ruairi.defrein@tudublin.ie

**Abstract**—This paper introduces a new time-resolved spectral analysis method based on the Linear Prediction Coding (LPC) method that is particularly suited to the study of the dynamics of EEG (Electroencephalography) activity. The spectral dynamics of EEG signals can be challenging to analyse as they contain multiple frequency components and are often corrupted by noise. The LPC Filtering (LPCF) method described here processes the LPC poles to generate a series of reduced-order filter transform functions which can accurately estimate the dominant frequencies. The LPCF method is a parameterized time-frequency method that is suitable for identifying the dominant frequencies of multiple-component signals (e.g. EEG signals). We define bias and the frequency resolution metrics to assess the ability of the LPCF method to estimate the frequencies. The experimental results show that the LPCF can reduce the bias of the LPC estimates in the low and high frequency bands and improved frequency resolution. Furthermore, the LPCF method is less sensitive to the filter order and has a higher tolerance of noise compared to the LPC method. Finally, we apply the LPCF method to a real EEG signal where it can identify the dominant frequency in each frequency band and significantly reduce the redundant estimates of the LPC method.

**Index Terms**—EEG analysis, modified linear predictive coding, time-frequency method.

## I. INTRODUCTION

EEG is an important bioelectrical signal for researchers to explore the diagnosis and treatment of mental [1] and brain neuron-degenerative diseases [2] and abnormalities [3]. Dynamically exploring the key spectral characteristic information in EEG signals via time-frequency analysis can help researchers to better understand human brain activity. Many of the traditional time-frequency methods are waveform methods such as the short-time Fourier transform [4] and the continuous wavelet transform [6]. These are excellent at demonstrating whether a certain frequency component exists or not by showing how the energy of the signal is distributed across the time-frequency domain. In this paper, we propose a LPCF method which is a parameterized time-frequency method and it can robustly and accurately identify the dominant frequencies of noisy signals in the different frequency bands. An EEG signal is a multiple components signal and it has adopted different frequency bands ( $\delta, \theta, \alpha, \beta, \gamma$ ) to analyse the different brain functions. The typical EEG signal is a high noise time-varying signal which requires the time-frequency method to be robust to noise. The LPCF method described here is particularly

suitable for studying the dynamics of the dominant frequency at different EEG bands.

The LPC method can give us a numerical estimation frequency result. It has been extensively applied in speech signal processing for formant frequency identification [5]. However, the standard LPC suffers from a sensitivity to noise and its performance is dependent on the filter order [8], [10]. In this paper, we propose a LPC Filtering method to further process the LPC poles into different frequency bands to generate a series of reduced-order filter transform functions to estimate the dominant frequency. The LPCF method is a further modification of our previous work [8], [9]. The LPCF method can overcome the shortcomings of the LPC method, namely a sensitivity to noise and the LPC order. We use the Monte Carlo simulation method to generate the Probability Density Function (PDF) and use the mean and standard deviation of the PDF to define the bias and frequency resolution of the method. These results show that (1) LPCF significantly reduces the bias of the LPC estimates in the low and high frequency bands; (2) LPCF can provide improved frequency resolution compared to LPC; (3) The LPCF method has a reduced sensitivity to the filter order and has a higher tolerance of noise than the LPC method. Furthermore, the LPCF method accurately identifies the dominant frequencies in the different frequency bands of an EEG signal.

This paper is organised as follows. In Section II, we first present details of the LPCF method. In Section III, we introduce the EEG frequency bands and the experimental metrics. Experimental results are presented in Section IV. Finally, the conclusions of the paper are presented in Section V.

## II. METHOD INTRODUCTION

The LPC algorithm provides a method for estimating the parameters that characterize the linear time-varying system [10]. It is based on the assumption that the current signal sample  $s(n)$  can be closely approximated as a linear combination of past samples

$$\hat{s}(n) = \sum_{i=1}^P a_i s(n-i), \quad (1)$$

where the factor  $a_i$  is the predictor coefficient and is determined by minimizing the mean-squared error between the actual samples  $s(n)$  and the predicted values  $\hat{s}(n)$ .

### A. LPC Method

The LPC analysis operates on frames containing data samples. In the  $z$ -transform domain, a  $P^{th}$  order linear predictor is a system of the form

$$L(z) = \sum_{i=1}^P a_i z^{-i} = \frac{\hat{S}(z)}{S(z)} \quad (2)$$

where  $\hat{S}(z)$  is the output of the filter. The  $z$ -transform for the prediction error can be written as

$$E(z) = S(z) - \sum_{i=1}^P a_i S(z) z^{-i}. \quad (3)$$

The prediction error is the output of a system with a transfer function

$$A(z) = \frac{E(z)}{S(z)} = 1 - L(z) = 1 - \sum_{i=1}^P a_i z^{-i} \quad (4)$$

where  $A(z)$  is an inverse filter for  $H(z)$  given by

$$H(z) = \frac{1}{A(z)} = \frac{1}{1 - \sum_{i=1}^P a_i z^{-i}}. \quad (5)$$

The fundamental theorem of algebra tells us that  $H(z)$  has  $P$  poles which are the values of  $z$  for which  $H(z) = \infty$ . Therefore in finding the poles of  $H(z)$  we obtain the set  $\{z_1, z_2, z_3, \dots, z_P\}$ . As each pole  $z_i$  is complex it can be expressed as

$$z_i = \gamma_i e^{j\omega_i}, \quad (i = 1, 2, 3, \dots, M) \quad (6)$$

where  $\omega_i = \tan^{-1}[\text{Im}(z_i)/\text{Re}(z_i)]$  is the angle corresponding to the pole. The magnitude of a pole is  $m_i = |z_i|$  and the corresponding pole frequency is

$$p_i = \frac{\omega_i}{2\pi T_s}, \quad (i = 1, 2, 3, \dots, M) \quad (7)$$

where  $T_s$  is the sample period. The poles of  $H(z)$  are often used to directly estimate the frequency content of signals [10] [16] [17]. The LPC method is the benchmark for our approach and the poles resulting from LPC are used as the frequency estimates for the analysed signals. Given that the poles occur in the filter as complex conjugate pole pairs, we only consider those poles with non-negative imaginary parts  $\text{Im}(z_i) \geq 0$  and the number of LPC estimates is denoted by  $M$ .

### B. LPCF Method

The proposed LPCF method further processes the LPC poles to generate a series of reduced-order transform functions to estimate the dominant frequencies in the different frequency bands. The details of further processing of LPC poles are as follows:

- 1) Obtain the set of poles of the LPC filter  $H(z)$ , i.e.  $\{z_1, z_2, z_3, \dots, z_M\}$  and partition the poles into different frequency bands.
- 2) Organise the poles of each frequency band into a dominant pole and local poles. The LPC pole with the

largest magnitude is classified as the dominant pole  $\tilde{z}_i$  and the number of dominant poles is  $N$ , other poles are the non-dominant poles. The non-dominant poles around the dominant poles are called local poles  $\hat{z}$  which can affect the final location of the spectral peak. A distance threshold  $\lambda$  is defined to identify the local poles. When the distance (frequency separation)  $\Delta f$  between the dominant poles  $\tilde{z}_i$  and non-dominant poles is less than  $\lambda$ , we consider these non-dominant poles to be the local poles  $\{\hat{z}_{i1}, \hat{z}_{i2}, \dots, \hat{z}_{iL}\}$  where the  $L$  is the number of local poles for  $i^{th}$  dominant pole.

- 3) The dominant pole and its local non-dominant pole(s) form a new reduced order transform function which is denoted

$$\tilde{H}_i(z) = \frac{1}{(1 - \tilde{z}_i^{-1})} \times \prod_{j=1}^L \frac{1}{(1 - \hat{z}_{ij}^{-1})}. \quad (8)$$

As the new filter transfer function  $\tilde{H}_i(z)$  has a lower order, it has fewer local maxima which makes it easier to find the peaks.

- 4) Estimate the dominant frequencies. The maximum peak  $\tilde{p}_i$  of the  $\tilde{H}_i(z)$  is the dominant frequency component of the  $i^{th}$  frequency band. So the estimates of the LPCF method are  $\{\hat{p}_1, \hat{p}_2, \dots, \hat{p}_N\}$ .

## III. PERFORMANCE EVALUATION METRICS

### A. EEG Frequency Bands

Many EEG research works have divided the spectra of EEG waveforms into several fixed frequency bands and are named based on their frequency range using Greek letters ( $\delta, \theta, \alpha, \beta, \gamma$ ). Different researchers have defined different frequencies for these bands with little consensus between them [11]–[15]. In this paper, we use the EEG frequency band standard from [12], as shown in Table I.

TABLE I  
EEG FREQUENCY BANDS.

Name of EEG Waves	$\delta$	$\theta$	$\alpha$	$\beta$	$\gamma$
Frequency Range (Hz)	0-4	4-8	8-12	13-30	over 30

### B. Metrics

LPCF is a parameterized method and a Monte Carlo simulation is used to generate the Error Probability Density Function (EPDF) to measure the bias of the estimates and to estimate the frequency resolution of the LPCF method. The Monte Carlo trials in all experiments of this paper are repeated 1000 times and the simulation signals are sinusoidal signals whose frequencies have a uniform random distribution. To ensure that we do not unfairly penalize the LPC method, we only considered the frequency estimates whose error was less than 5 Hz from the true frequency in the experimental evaluation conducted in this paper. In this paper, we define the mean value of the EPDF as the bias of the method. A histogram of the frequency errors where the error  $e$  range is from -5 Hz to +5

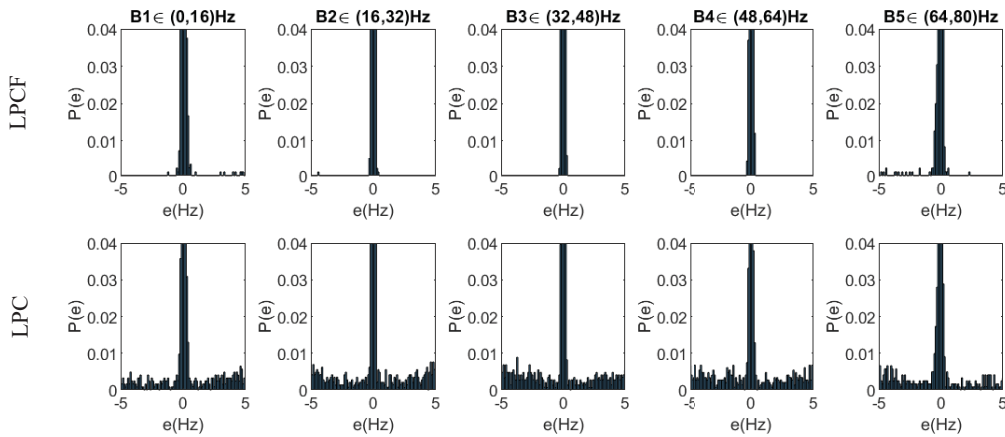


Fig. 1. The EPDF of the LPCF method and LPC method under the different frequency bands. The y-axis of each EPDF is fixed from 0 to 0.04 to zoom the EPDF so that it easier to observe the low  $P(e)$  in EDPF.

Hz and the bin size is 0.1 Hz. For each histogram bar, we start by multiplying the central error value by the corresponding bar height and the height of each histogram bar is expressed as a probability  $P(e)$  (i.e. to ensure  $\sum P(e) = 1$ ). The bias is defined as

$$\mu = \sum eP(e), \quad (9)$$

where the  $\mu$  is the bias of the all estimates. The standard deviation  $\sigma$  of the EPDF is used to measure the frequency resolution of the LPC-based method. The frequency resolution  $\Delta f$  is defined as

$$\Delta f = \sigma = \sqrt{\sum (e - \mu)^2 P(e)} \quad (10)$$

The Heisenberg-Gabor uncertainty principle tells us what can be achieved with regard to time-frequency localization for the short-time Fourier transform [7], by referring to the dimensions of the tiles ( $\Delta t \times \Delta f$ ) in the time-frequency plane. Therefore, the Time-Bandwidth Product (TBP) of the LPC-based method is

$$TBP = \Delta f \times \Delta t \quad (11)$$

where  $\Delta t$  represents the time resolution.

TABLE II  
THE FREQUENCY RANGE OF DIFFERENT FREQUENCY BANDS.

Label	B1	B2	B3	B4	B5
Frequency Range (Hz)	0-16	16-32	32-48	48-64	64-80

#### IV. EXPERIMENTAL RESULTS

In this section, the first three experiments are Monte Carlo experiments where the experimental signals are sinusoidal signals with uniformly random frequency distribution. The last experiment applies the LPCF method to a real EEG signal.

##### A. Frequency Bands Analysis

In the first experiment, we analyze the EPDF of the LPCF and LPC methods in the different frequency bands. The sampling frequency of the simulation signal is  $f_s = 160$  Hz and the time resolution is  $\Delta t = 1$  s. The frequency domain is equally divided into 5 frequency bands (i.e. B1, B2, B3, B4 and B5). The details of the frequency bands are shown in Table II. The bands B1 and B2 correspond to low frequencies, B3 corresponds to middle frequencies, B4 and B5 correspond to high frequencies. The experimental signals are sinusoidal signals whose frequencies are uniform distribution for each frequency band. In order to simulate a high noise environment, Additive White Gaussian Noise (AWGN) is used to perturb the signal. The Signal-to-Noise Ratio (SNR) in dB is defined as the ratio of the power of the signal to the AWGN power. The SNR of this experiment is 3 dB, the order of the filters is  $P = 15$  and  $\lambda = 5$  Hz.

The EPDF results are shown in Fig. 1. The spread of EPDF of the LPC method is greater than that of the LPCF method within each frequency band. For the bias analysis in Fig. 2, the bias  $\mu$  of the LPC method is greater than 0 in the low frequency band (i.e. B1) and is less than 0 in the high frequency band (i.e. B5). This indicates that the LPC method overestimates the frequency in the low frequency band and underestimates the frequency in the high frequency band. The LPCF method can reduce this bias of the LPC method.

For the frequency resolution analysis in Fig. 3, the LPC method has a lower frequency resolution in the middle band. The reason is that the estimates of the LPC method in the low and high frequency bands are biased to one side, while the EPDF in the middle frequency band is not biased, thus causing the  $\Delta f$  in the middle frequency band to be higher than in other frequency bands. This is also one of the reasons why the LPC method has a larger bias in the high and low frequency bands than in the middle band. For the LPCF method, it can provide a better frequency resolution than that of LPC in the different frequency bands. The details of TBP are shown in

Table III. The TBP value of the LPCF method is much lower than that of the LPC method. This result is consistent with the result of the bias analysis in Fig. 3 when the time resolution is fixed. In the following experiments (i.e. subsection IV-B and IV-C), we focused on selecting three representative frequency bands for detailed analysis, namely, B1 represents the high frequency band, B3 represents the middle frequency band, and B5 represents the high frequency band.

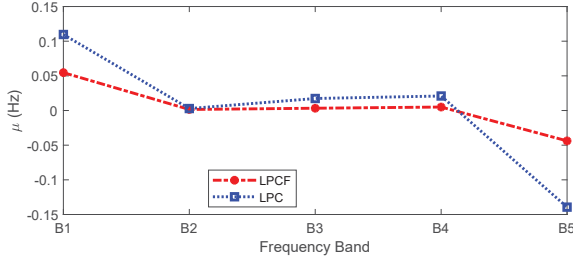


Fig. 2. The bias of the LPCF and LPC methods for different frequency bands.

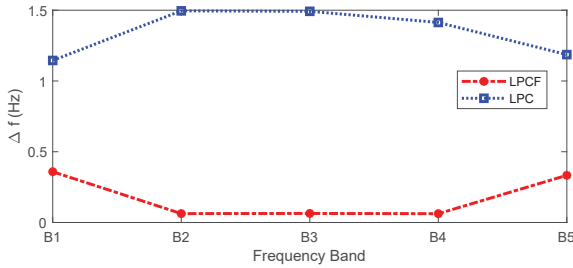


Fig. 3. The frequency resolution of the LPCF and LPC methods for different frequency bands.

TABLE III  
LPCF vs LPC: THE TBP FOR THE DIFFERENT FREQUENCY BANDS.

Frequency Band	B1	B2	B3	B4	B5
TBP(LPCF)	0.3587	0.0628	0.0640	0.0622	0.3334
TBP(LPC)	1.1450	1.4955	1.4923	1.4134	1.1863

### B. LPC Order Analysis

In this experiment, we analyse the influence of the LPC order on the bias and frequency resolution of the two methods. The filter order  $P$  is changed from 5 to 25 and the step size is 5. The SNR of the signal is 3 dB and the other experimental parameters are the same as those used in the previous subsection. Fig. 4 and Fig. 5 show the bias analysis and the frequency resolution of LPCF and LPC for different filter orders. As we can see in Fig. 4, the bias  $\mu$  of the LPC method in the low frequency band is greater than 0 and in the high frequency band is less than 0. This indicates the LPC method has a larger bias in the low and high frequency bands than in the middle frequency band. The bias  $\mu$  (Fig. 4) and the  $\Delta f$  (Fig. 5) of the LPC method first decreases and then increases with the increase of LPC order. The LPC method has the smallest bias value at  $P = 15$  and it has the smallest  $\Delta f$

at  $P = 10$ . These results indicate the performance of the LPC method is dependent on the filter order. For the LPCF method, it can provide a smaller bias than the LPC method after  $P$  is greater than 10. The reason is that the filter order is too low to provide sufficient spectral information when  $P = 5$ . In Fig. 5, the LPCF method has a high frequency resolution under different filter orders and are not affected by the filter order. So the performance of the LPCF method is less sensitive to the filter order than that of the LPC method. Table IV shows the TBP results of this experiment in which the LPCF values are less than the LPC for all cases.

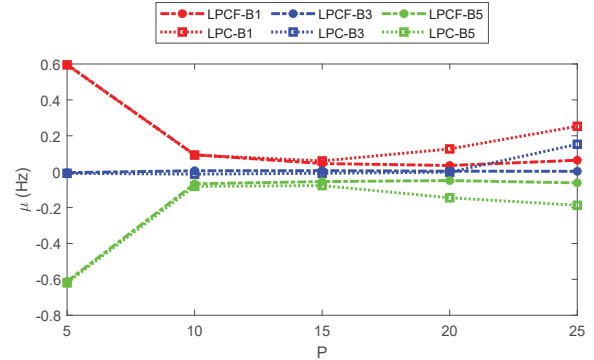


Fig. 4. The bias of the LPCF and the LPC methods for different filter orders.

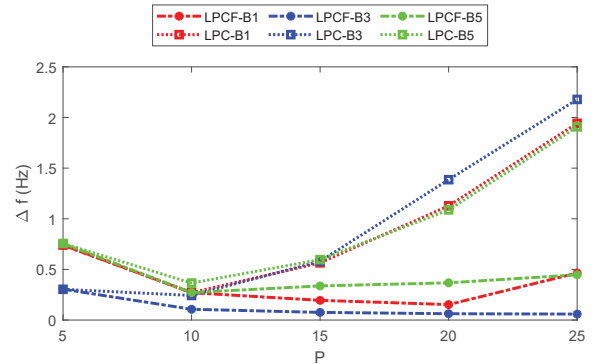


Fig. 5. The frequency resolution of the LPCF and LPC methods for different filter orders.

TABLE IV  
LPCF vs LPC: THE TBP FOR DIFFERENT FILTER ORDER.

LPC order		5	10	15	20	25
B1(TBP)	LPCF	0.7398	0.2702	0.1945	0.1529	0.4639
	LPC	0.7399	0.2707	0.5647	1.1282	1.9428
B3(TBP)	LPCF	0.3036	0.1065	0.0756	0.0624	0.0588
	LPC	0.3049	0.2426	0.5803	1.3860	2.1785
B5(TBP)	LPCF	0.7558	0.2712	0.3370	0.3677	0.4467
	LPC	0.7559	0.3650	0.5968	1.0877	1.9075

### C. Signal Noise Analysis

In this experiment, we analyse the effect of noise on the two methods. The LPC order  $P = 15$  and other experimental parameters are the same as the experiment in the previous



subsection. Fig. 6 and Fig. 7 demonstrate the bias  $\mu$  and  $\Delta f$  of the LPCF method and LPC method under different SNR conditions. We can see that LPCF has a smaller  $\mu$  than LPC under the same SNR level and LPCF can provide a higher frequency resolution than that of LPC for the same SNR level. In Fig. 7, the  $\Delta f$  of the LPC method becomes larger as the SNR is increased. The reason is that the range of EPDF only analyses frequency errors less than 5 Hz. But the error of estimates of the LPC method is over 5 Hz when the signal has a low SNR. So only the errors between the -5 and 5 Hz are counted which is why the  $\mu$  and  $\Delta f$  of the LPC method become greater as the SNR increases. Fig. 8 and Fig. 9 show the results when the error range extends from -15 to 15 Hz. Fig. 8 shows that the bias of both methods is decreased as the SNR increases and Fig. 9 shows that the  $\Delta f$  of both methods is decreased as the SNR increases. The bias of the LPCF method still is much lower than that of LPC and the frequency resolution is much lower than that of LPC at B3. These results show that LPCF method has a higher tolerance to noise than LPC. Table V shows the TBP values of the LPC method and LPCF method and the error range of EPDF is from -5 to 5 Hz. In short, the TBP value of LPCF is lower than the LPC method for the different SNR levels.

TABLE V  
LPCF vs LPC: THE TBP UNDER DIFFERENT SNR LEVELS.

SNR(dB)		0	3	6	9	12
B1(TBP)	LPCF	0.3195	0.2497	0.1385	0.2779	0.2681
	LPC	0.5363	0.6414	0.7316	0.8568	1.3547
B3(TBP)	LPCF	0.1200	0.0734	0.0527	0.0388	0.0202
	LPC	0.6966	0.7367	0.9320	1.3950	1.6848
B5(TBP)	LPCF	0.2223	0.1892	0.3631	0.1957	0.1790
	LPC	0.5469	0.4649	0.7195	0.9631	1.2289

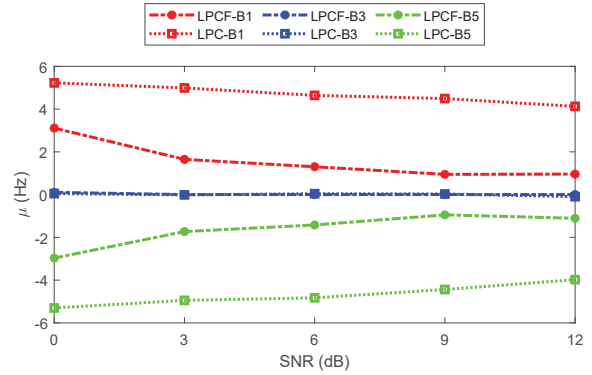


Fig. 8. The bias of the the LPCF and LPC methods under different SNR where the error range extends from -15 to 15 Hz.

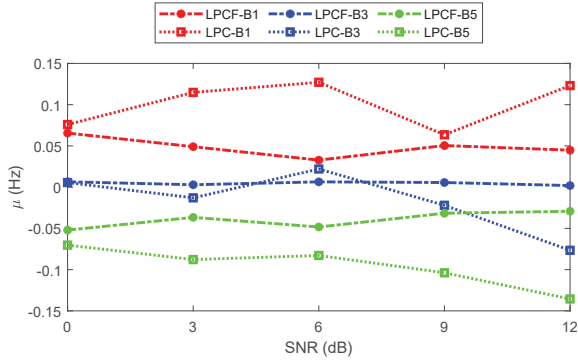


Fig. 6. The bias of the LPCF and LPC methods under the different SNR.

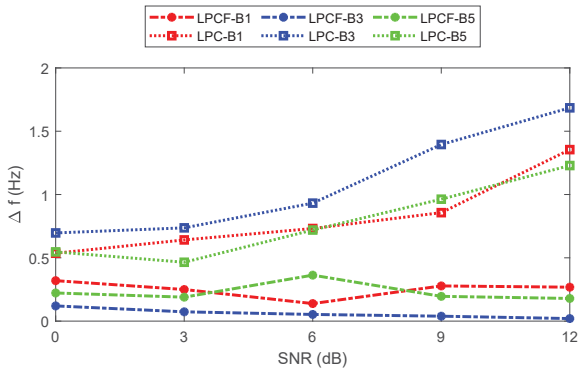


Fig. 7. The frequency resolution of the LPCF and LPC methods under the different SNR.

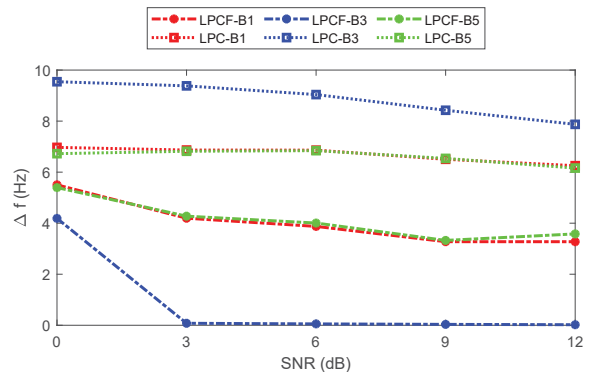
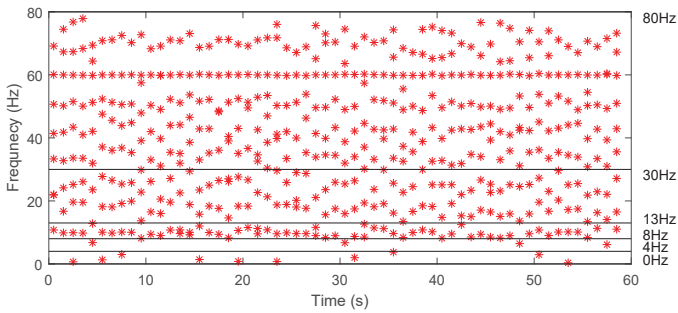


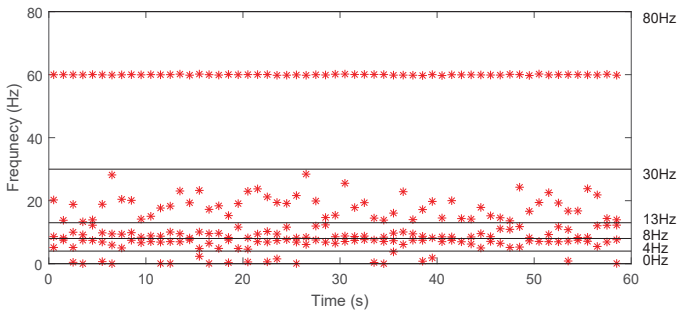
Fig. 9. The frequency resolution of the LPCF and LPC methods under different SNR where the error range extends from -15 to 15 Hz.

#### D. EEG Analysis

In this experiment, we demonstrate a real EEG signal application using LCP and LPCF to identify the dominant frequency components of different EEG waves ( $\delta, \theta, \alpha, \beta, \gamma$ ). The EEG signal used in our experiment comes from the public dataset BCI2000 [18]. The sampling frequency of the EEG signal is  $f_s=160$  Hz, the length of the EEG is 60 s. The order of LPC  $P=20$ , the time resolution  $\Delta t = 1$  s. Other experimental parameters are the same as the experiments in the previous subsection. Fig. 10 compares the frequency estimations response between LPC and LPCF method. The black line is the reference line for different EEG frequency bands. It is particularly noticeable that both LPC and LPCF methods have identified the AC power supply frequency of 60 Hz. The LPC method directly generates many estimation



(a) LPC Method



(b) LPCF Method

Fig. 10. Comparing time-resolved spectra of the LPC and LPCF methods in a EEG signal. The x-axis is the time. The left y-axis is the frequency. The right y-axis is the boundary value of EEG frequency band. The black line is the boundary line of different EEG frequency bands.

frequencies as it does not distinguish between the dominant and non-dominant poles. These results show that LPCF has a greater ability to estimate the dominant frequency in different frequency bands than LPC. The LPCF method can reduce the bias of LPC in the same frequency band and it can provide higher frequency resolution at the same time resolution as the LPC method. The LPCF method allows us to estimate the dominant frequency component in each of the EEG bands and it can track the dominant frequency changes of the different EEG frequency bands.

## V. CONCLUSION

This paper introduces a parameterized time-frequency method LPCF which further processes the LPC poles to generate a series of reduced-order filter transform functions to estimate the dominant frequency at different frequency bands. Definitions of the bias and the frequency resolution are introduced to analyse the performance of the LPCF method. The experimental results show that the LPCF method can significantly reduce the bias of the LPC method in the low and high frequency bands. It can provide higher frequency resolution than LPC in different frequency bands and different filter orders. LPCF is a robust method which is less sensitive to the filter order and has a higher tolerance of noise than LPC. As EEG is a noisy multi-component signal, LPCF is particularly suited to study the dynamics of EEG activity where it can estimate the dominant frequencies in the different

EEG frequency bands. In further work, the LPCF method will be used to support further processing of the EEG signal using machine learning techniques.

## ACKNOWLEDGMENT

This work has been supported through the Graduate School of Technological University Dublin and this publication has emanated from research conducted with the financial support of Science Foundation Ireland (SFI) under the Grant Number 15/SIRG/3459.

## REFERENCES

- [1] Smith, S. J. M. "EEG in the diagnosis, classification and management of patients with epilepsy." *Journal of Neurology, Neurosurgery and Psychiatry* 76.suppl 2 (2005): ii2-ii7.
- [2] Yoshikawa, Toshikazu, Yuji Naito, and Motoharu Kondo. "Ginkgo biloba leaf extract: review of biological actions and clinical applications." *Antioxidants and redox signaling* 1.4 (1999): 469-480.
- [3] Wang, Jun, et al. "Resting state EEG abnormalities in autism spectrum disorders." *Journal of neurodevelopmental disorders* 5.1 (2013): 1-14.
- [4] Griffin, Daniel, and Jae Lim. "Signal estimation from modified short-time Fourier transform." *IEEE Transactions on acoustics, speech, and signal processing* 32.2 (1984): 236-243.
- [5] de Frin, Ruair. "Power-Weighted LPC Formant Estimation." *IEEE Transactions on Circuits and Systems II: Express Briefs* (2020): 1-1.
- [6] AguiarConraria, Lus, and Maria Joana Soares. "The continuous wavelet transform: Moving beyond uniaid bivariate analysis." *Journal of Economic Surveys* 28.2 (2014): 344-375.
- [7] Gabor, Dennis. "Theory of communication. Part 1: The analysis of information." *Journal of the Institution of Electrical Engineers-Part III: Radio and Communication Engineering* 93, no. 26, 1946, pp. 429-441.
- [8] Xu, Jin, Mark Davis, and Ruairí de Fréin. "New Robust LPC-Based Method for Time-resolved Morphology of High-noise Multiple Frequency Signals." *PIIn 2020 31st Irish Signals and Systems Conference (ISSC)*, pp. 1-6, Jun 2020.
- [9] Xu, Jin, Mark Davis, and Ruairí de Fréin. "An LPC pole processing method for enhancing the identification of dominant spectral features." *Electronics Letters*, Jun 2021.
- [10] Duncan, G., and M. A. Jack. "Formant estimation algorithm based on pole focusing offering improved noise tolerance and feature resolution." *IEE Proceedings F (Communications, Radar and Signal Processing)*. Vol. 135. No. 1. IET Digital Library, 1988, pp. 18-32.
- [11] Deuschl, Gntner. "Recommendations for the practice of clinical neurophysiology." *guidelines of the International Federation of Clinical Neurophysiology* (1999).
- [12] Adeli, Hojjat, Samanwoy Ghosh-Dastidar, and Nahid Dadmehr. "A wavelet-chaos methodology for analysis of EEGs and EEG subbands to detect seizure and epilepsy." *IEEE Transactions on Biomedical Engineering* 54.2 (2007): 205-211.
- [13] Ferri, Raffaele, et al. "The functional connectivity of different EEG bands moves towards small-world network organization during sleep." *Clinical Neurophysiology* 119.9 (2008): 2026-2036.
- [14] Abo-Zahhad, M., Sabah M. Ahmed, and Sherif N. Abbas. "A new EEG acquisition protocol for biometric identification using eye blinking signals." *International Journal of Intelligent Systems and Applications* 7.6 (2015): 48.
- [15] Zheng, Wei-Long, and Bao-Liang Lu. "Investigating critical frequency bands and channels for EEG-based emotion recognition with deep neural networks." *IEEE Transactions on Autonomous Mental Development* 7.3 (2015): 162-175.
- [16] Manolakis, Dimitris G., Vinay K. Ingle, and Stephen M. Kogon. "Statistical and adaptive signal processing: spectral estimation, signal modeling, adaptive filtering, and array processing." 2000.
- [17] Barnwell, T. III, Kambiz Nayebi, and Craig Richardson. "Speech Coding: A Computer Laboratory Textbook." *Computers and Mathematics with Applications* 11.31, 1996, pp. 139.
- [18] Schalk, Gerwin, et al. "BCI2000: a general-purpose brain-computer interface (BCI) system." *IEEE Transactions on biomedical engineering* 51.6 (2004): 1034-1043.